View metadata, citation and similar papers at core.ac.uk
brought to you by CORE
provided by Elsevier - Publisher Connector

Cell Stem Cell
Article

MicroRNA Regulation of Cell Lineages in Mouse and Human Embryonic Stem Cells

Kathryn N. Ivey,[1,2,3] Alecia Muth,[1,2,3] Joshua Arnold,[1,2,3] Frank W. King,[2] Ru-Fang Yeh,[4] Jason E. Fish,[1,2,3] Edward C. Hsiao,[1,5] Robert J. Schwartz,[7] Bruce R. Conklin,[1,5,6] Harold S. Bernstein,[2] and Deepak Srivastava[1,2,3,*]
[1]Gladstone Institute of Cardiovascular Disease
[2]Department of Pediatrics
[3]Department of Biochemistry and Biophysics
[4]Department of Epidemiology and Biostatistics
[5]Department of Medicine
[6]Department of Molecular and Cellular Pharmacology
University of California, San Francisco, 1650 Owens Street, San Francisco, CA 94158, USA
[7]Institute of Biosciences and Technology, Texas A&M Health Science Center, Houston, TX 77030, USA
*Correspondence: dsrivastava@gladstone.ucsf.edu
DOI 10.1016/j.stem.2008.01.016

SUMMARY

Cell fate decisions of pluripotent embryonic stem (ES) cells are dictated by activation and repression of lineage-specific genes. Numerous signaling and transcriptional networks progressively narrow and specify the potential of ES cells. Whether specific microRNAs help refine and limit gene expression and, thereby, could be used to manipulate ES cell differentiation has largely been unexplored. Here, we show that two serum response factor (SRF)-dependent muscle-specific microRNAs, miR-1 and miR-133, promote mesoderm formation from ES cells but have opposing functions during further differentiation into cardiac muscle progenitors. Furthermore, miR-1 and miR-133 were potent repressors of nonmuscle gene expression and cell fate during mouse and human ES cell differentiation. miR-1's effects were in part mediated by translational repression of the Notch ligand Delta-like 1 (Dll-1). Our findings indicate that muscle-specific miRNAs reinforce the silencing of nonmuscle genes during cell lineage commitment and suggest that miRNAs may have general utility in regulating cell-fate decisions from pluripotent ES cells.

INTRODUCTION

Embryonic stem (ES) cells, derived from the inner cell mass of blastocysts, are pluripotent and self-renewing cells with the unique ability to give rise to all three germ layers—ectoderm, mesoderm, and endoderm. Precise regulation of cell-fate decisions is a prerequisite for future therapeutic use of ES cells. Numerous signaling pathways, including those involving members of the Wnt, Bmp, and Notch pathways, appear to regulate cell fate during embryogenesis and can be utilized in various forms to influence lineage choices in cultured ES cells (reviewed in Loebel et al., 2003). Such pathways often culminate in transcriptional events, through either DNA-binding proteins or chromatin-remodeling factors that dictate which subset of the genome is activated or silenced in specific cell types. As a result, transcription factors that regulate pluripotency or lineage-specific gene and protein expression have been a major focus of ES cell research.

In addition to transcriptional regulation, posttranscriptional control by small noncoding RNAs, such as microRNAs (miRNAs), quantitatively influences the ultimate proteome (He and Hannon, 2004; Ambros, 2004). miRNAs are naturally occurring RNAs that are transcribed in the nucleus, often under the control of specific enhancers, and are processed by the RNases Drosha/DGCR8 and Dicer into mature ~22 nucleotide RNAs that bind to complementary target mRNAs. miRNA:mRNA interactions in RNA-induced silencing complexes can result in mRNA degradation, deadenylation, or translational repression at the level of the ribosome. Over 450 human miRNAs have been described, and each is predicted to target tens if not hundreds of different mRNAs. Because they can regulate numerous genes, often in common pathways, miRNAs are candidates for master regulators of cellular processes, much like transcription factors that regulate entire programs of cellular differentiation and organogenesis (Zhao and Srivastava, 2007).

As pluripotent cells adopt particular fates, genes are transcriptionally activated that specify lineages. For ES-derived cell types, it is equally critical to suppress the expression of genes that would otherwise drive differentiation toward alternative fates. While this occurs at the transcriptional level, it is possible that miRNAs also contribute to this process by clearing latently expressed mRNAs as cells activate expression profiles reflecting their newly adopted fates. Indeed, ES cells lacking Dicer or Drosha, and therefore most mature miRNAs, cannot differentiate into most lineages (Kanellopoulou et al., 2005; Murchison et al., 2005; Wang et al., 2007). Although ES cell-specific miRNAs have been described (Houbaviy et al., 2003), the function or potential of specific miRNAs in ES cell differentiation has not been reported.

During differentiation of ES cells into aggregates called embryoid bodies (EBs), which to a limited extent recapitulate embryonic development, cardiomyocytes are among the first cell types

to arise. They become easily visible 7 days after differentiation as small clusters of rhythmically and synchronously contracting cells. Like naturally occurring cardiac muscle cells, ES cell-derived cardiomyocytes express markers of cardiac differentiation, assemble contractile machinery, and establish cell-cell communication (Maltsev et al., 1994).

In addition to the numerous transcription factors and signaling molecules that control development of cardiac cells (Srivastava, 2006), miRNAs have a critical role in cardiac differentiation in vivo (Zhao et al., 2005; Kwon et al., 2005; Zhao et al., 2007). In particular, miR-1 and miR-133 are cardiac and skeletal muscle-specific, bicistronic miRNAs that are transcriptionally controlled by some of the major regulators of muscle differentiation: serum response factor (SRF), MyoD, and Mef2 (Zhao et al., 2005; Kwon et al., 2005; Sokol and Ambros, 2005; Rao et al., 2006). miR-1 promotes differentiation of cardiac progenitors and exit from the cell cycle in mammals and in flies (Zhao et al., 2005, 2007; Kwon et al., 2005). In contrast, miR-133 inhibits differentiation of skeletal myoblasts and maintains them in a proliferative state (Chen et al., 2006). Several direct targets of miR-1 have been described in vivo (Zhao et al., 2005; 2007), including Hand2, a transcription factor required for expansion of cardiac progenitors (Srivastava et al., 1997; Yamagishi et al., 2001), and the Notch ligand *delta* in *Drosophila* (Kwon et al., 2005).

Here, we show that miR-1 and miR-133 are enriched in ES cell-derived cardiomyocytes and are expressed at the early stages of cardiac mesoderm selection from ES cells. Expression of either miR-1 or miR-133 in ES cells resulted in enhanced mesoderm gene expression in differentiating EBs but suppressed differentiation into the ectodermal or endodermal lineages. However, miR-1 and miR-133 had opposing effects on further adoption of muscle lineages, with miR-1 promoting and miR-133 blocking differentiation into either cardiac or skeletal muscle fates. Delta-like 1 (Dll-1), a Notch ligand expressed in ES cells, was translationally repressed in miR-1-expressing ES cells, and depletion of Dll-1 from ES cells resulted in a bias toward the cardiac lineage while suppressing endoderm and neuroectoderm differentiation, similar to miR-1-expressing ES cells. Our findings demonstrate that miRNAs can control cell lineage determination from pluripotent ES cells, likely by fine-tuning the transcriptome of differentiating cells during commitment to a newly adopted fate.

RESULTS

miRNA Expression in Mouse ES Cells and ES Cell-Derived Cardiomyocytes

To determine which miRNAs are enriched during differentiation of mouse ES (mES) cells into cardiomyocytes, we used a mES cell line carrying a green fluorescent protein (GFP) transgene under control of the β-myosin heavy-chain promoter, which is uniquely expressed in differentiated cardiomyocytes. We isolated RNA from GFP$^+$ and GFP$^-$ cells by fluorescence-activated cell sorting after 13 days of EB differentiation and profiled miRNA expression by microarray analysis. Seventeen miRNAs were enriched at least 3-fold in the GFP$^+$ population (Figure 1A). Approximately half of the miRNAs that were enriched in mES cell-derived cardiomyocytes, including the muscle-specific miRNAs miR-1 and miR-133, were undetectable in undifferentiated mES cells, indicating that they were unique to differentiating cells (Figure 1A).

A

	Fold Enrichment in βMHC-GFP$^+$ Cells	Detected in mES Cells
miR-143	12.1	–
miR-295	9.0	+
miR-200a	8.6	–
miR-24	7.2	–
miR-1	6.7	–
miR-182	6.2	+
miR-133	5.4	–
miR-18	5.1	+
miR-26a	5.0	–
miR-335	5.0	–
miR-23b	4.1	+
miR-183	3.7	–
miR-30c	3.7	+
miR-200b	3.8	–
miR-292-3p	3.6	+
miR-293	3.4	+
miR-20	3.2	+

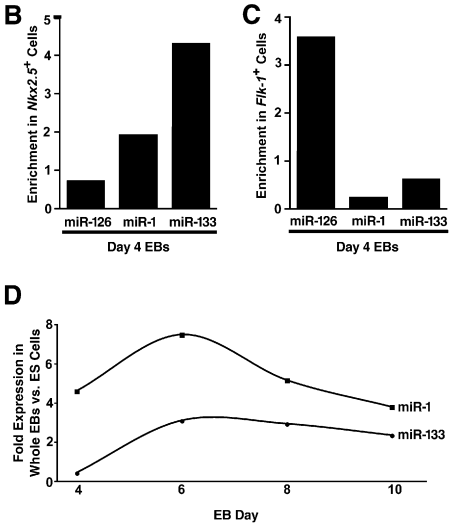

Figure 1. Identification of miRNAs Expressed in ES Cell-Derived Cardiomyocytes

(A) mES cells carrying a *GFP* transgene under control of the cardiomyocyte-specific β-myosin heavy chain promoter were differentiated for 13 days as embryoid bodies (EBs), sorted by GFP expression, and analyzed by miRNA microarray. miRNAs enriched at least threefold in the GFP$^+$ compared to GFP$^-$ cell populations are listed along with their fold enrichment and whether they were detected in ES cells.

(B and C) Quantitative RT-PCR (qRT-PCR) showing enrichment of miR-1 and miR-133 in flow-sorted Nkx2.5-GFP$^+$ cardiac progenitors from day 4 EBs (B), but not in Flk-1$^+$ vascular progenitors, which are enriched in the endothelial-specific miRNA, miR-126 (C).

(D) qRT-PCR showing expression kinetics of miR-1 and miR-133 during days 4–10 of EB differentiation.

To determine whether miR-1 and miR-133 were present and enriched in early cardiac progenitors, we utilized a mES cell line carrying a *GFP* transgene under transcriptional control of a recombinant bacterial artificial chromosome containing the *Nkx2.5* enhancer (B.R.C., Y. Yoshinaga, T.D. Nguyen, S.L. Musone, J.E. Kim, P. Swinton, I. Espineda, C. Manalac, P.J. deJong, and E.C.H., unpublished data). This line effectively marks the early emergence of precardiac mesoderm. Sorting of GFP-positive cells in day 4 EBs followed by quantitative RT-PCR (qRT-PCR) revealed that the muscle-specific miRNAs were expressed

specifically in the early precardiac mesoderm at this early stage (Figure 1B), while the vascular endothelium-enriched miRNA, miR-126, was absent (Kuehbacher et al., 2007). Conversely, when we sorted vascular progenitors from day 4 EBs based on their cell surface expression of Flk-1, miR-1 and miR-133 were absent from the Flk-1$^+$ mesoderm population in which miR-126 was highly expressed (Figure 1C). We also examined the kinetics of miR-1/miR-133 expression in differentiating whole EBs (Figure 1D). Both were detectable as early as day 4, and their expression increased until day 6, after which their relative abundance in the growing EBs diminished and other cell types emerged.

miR-1 and miR-133 Can Promote Mesoderm Differentiation in mES Cells

Since miR-1 and miR-133 were not expressed in undifferentiated mES cells but were specifically enriched in precardiac mesoderm, we hypothesized that their introduction into mES cells might bias cells toward a muscle lineage. Lentiviruses were used to infect and select ES cell lines expressing miR-1 (mES$^{miR\text{-}1}$) or miR-133 (mES$^{miR\text{-}133}$) (Figure 2A). The levels of introduced miRNAs approximated those of the endogenous miRNAs in the mouse heart (Figure 2B). The morphology (data not shown) and doubling time of the cell lines in LIF-containing medium were unaltered (Figure 2C), and the pluripotency markers *Oct-4* and *Nanog* were expressed at normal levels (data not shown).

To assess the lineage potential of mES cells expressing miR-1 and miR-133, we differentiated control, mES$^{miR\text{-}1}$, and mES$^{miR\text{-}133}$ cells by the hanging drop method; collected the resulting EBs on days 4, 6, and 10 of differentiation; and examined the expression of lineage markers by qRT-PCR. Since miR-1 and miR-133 were normally expressed in day 4 precardiac mesoderm, we examined expression of the early mesoderm marker, *Brachyury* (*Bry*). *Bry* expression was detected transiently in control EBs at day 4 and then rapidly declined (Figure 2D and data not shown). In day 4 EBs expressing miR-1 or miR-133, *Bry* expression was dramatically enhanced (Figure 2D), suggesting that both can promote mesodermal gene expression in pluripotent mES cells.

To determine the effects of miR-1 and miR-133 on further differentiation, we examined expression of *Nkx2.5*, a transcription factor that is one of the earliest cardiac markers (Figure 2E). In control EBs, *Nkx2.5* expression was detected by day 6 and was maintained at day 10. Expression of miR-1 increased *Nkx2.5* expression at day 6; by day 10, it was ~7-fold greater than in control EBs. Strikingly, expression of miR-133 blocked induction of *Nkx2.5* at both time points. We performed a similar expression analysis of *Myogenin*, an early skeletal muscle marker, to determine the effects of miR-1 and miR-133 on skeletal muscle differentiation. qRT-PCR analysis of *Myogenin* expression in day 4, 6, or 10 EBs revealed that miR-1, but not miR-133, markedly enhanced *Myogenin* expression (Figure 2F).

The increase in *Nkx2.5* expression, as assessed by qRT-PCR, may represent either an increase in the amount of *Nkx2.5* expressed per cell or in the number of cells expressing *Nkx2.5*. To distinguish between these two possibilities, we infected the *Nkx2.5-GFP* mES line with control, miR-1-, or miR-133-expressing lentivirus; selected with antibiotic; and differentiated these cells for 10 days. GFP was expressed in more miR-1-expressing EBs, and at higher levels per cell, than in wild-type EBs, and was almost undetectable in miR-133-expressing cells (Figure 2G). Thus, miR-1 appears to promote the emergence of both cardiac and skeletal progenitors in mES cells, while miR-133 does not enhance further differentiation of mesoderm precursors into either lineage.

miR-1 or miR-133 Can Rescue Mesoderm Gene Expression in *SRF*$^{-/-}$ EBs

Efficient methods for stable miRNA knockdown studies in differentiating EBs are not yet available due to the rapid doubling time of ES cells. However, we previously showed that expression of the miR-1/miR-133 locus in embryonic mouse hearts is directly dependent on SRF (Zhao et al., 2005). Therefore, we sought to use *SRF*$^{-/-}$ ES cells (Niu et al., 2005) as a model for complementation experiments that might reveal the specific contribution of these miRNAs within *SRF*$^{-/-}$ cells (Zhao et al., 2005). We found that *SRF*$^{-/-}$ EBs failed to activate miR-1 or miR-133 (Figure 2H), confirming the SRF dependency in the ES cell system, consistent with in vivo observations. Differentiation of mesodermal progenitors in EBs lacking *SRF* is weak and delayed (Weinhold et al., 2000). To our surprise, however, *Bry* expression persisted in *SRF*$^{-/-}$ EBs, even after 10 days of differentiation, reflecting delayed or arrested differentiation of mesodermal progenitors that normally downregulate *Bry* by day 5 (Figure 2I). Despite the many genes dysregulated in *SRF*$^{-/-}$ EBs, reintroduction of miR-1 in *SRF*$^{-/-}$ ES cells rescued the abnormal accumulation of *Bry*$^+$ progenitors at day 10 of differentiation, with *Bry* levels returning close to wild-type levels. Introduction of miR-133 had an intermediate effect on the level of *Bry* expression at day 10, but Bry levels were still significantly decreased. *SRF*$^{-/-}$ ES cells also displayed elevated expression of *Mesp1*, a marker of nascent cardiac mesoderm that is usually downregulated as differentiation progresses (Saga et al., 1996), and this was similarly corrected by reintroduction of miR-1 or miR-133 (Figure 2I). These data suggest miR-1 and, to a lesser degree, miR-133 can promote the progression of mesodermal progenitors and that the arrest of mesodermal progenitors in the absence of SRF may be largely due to the absence of this family of miRNAs.

Consistent with the changes in *Bry* expression, expression of miR-1 or miR-133 restored the expression of a number of mesodermal genes in day 10 *SRF*$^{-/-}$ EBs (Figure 2J). Blood cell–specific genes, such as *Cd53*, *CxCl4*, and *Thbs1*, were dramatically downregulated in *SRF*$^{-/-}$ EBs, reflecting the loss of hematopoeitic lineages in the absence of SRF. However, their expression was reinitiated upon reintroduction of miR-1 or miR-133, likely representing relief of the block to mesodermal differentiation. Even expression of *Mef2c*, a major regulator of muscle lineages (Molkentin et al., 1995), was restored by miR-1 and, to a lesser extent, by miR-133.

miR-1 and miR-133 Suppress Endoderm Differentiation in mES Cells

It has been proposed that in some contexts miRNAs function in a "fail-safe" mechanism to clear latent gene expression by targeting pathways that should not be activated in a particular cell type (Hornstein et al., 2005). Therefore, we investigated whether miR-1 and miR-133 might not only promote muscle lineage decisions but also reinforce them by repressing

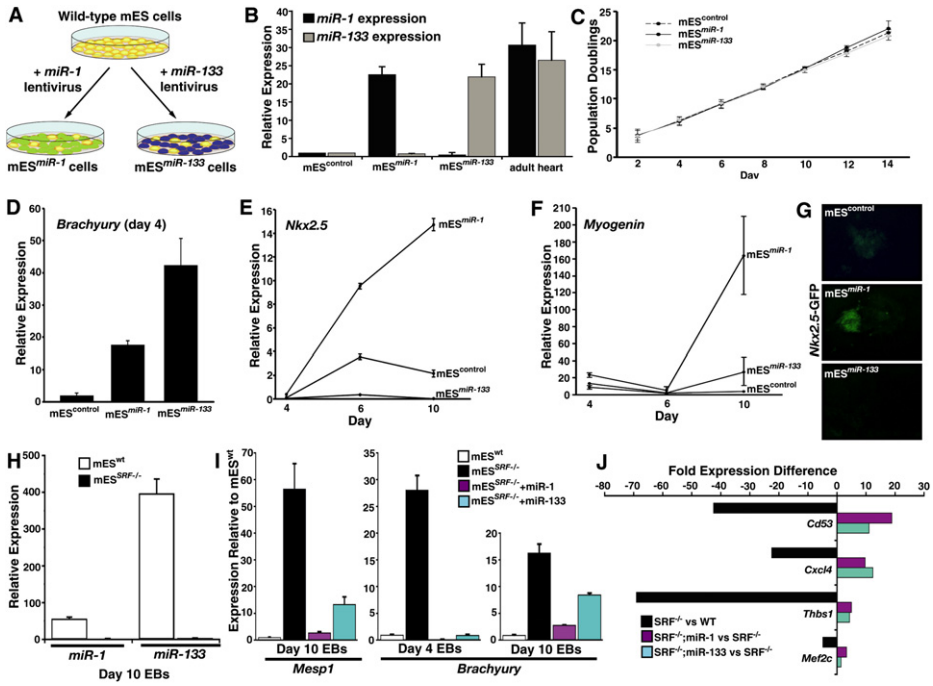

Figure 2. Effects of miR-1 and miR-133 on Mesoderm Differentiation

(A) Schematic of methods used to express miRNAs in mES cells. mES cells were infected with lentiviruses expressing miR-1 or miR-133 under control of a heterologous *EF-1* promoter. Stably infected cells were selected based on their resistance to blasticidin to generate stable miRNA-expressing mES cell lines (mES^{miR-1} and mES$^{miR-133}$).

(B) qRT-PCR results confirmed the expression of miR-1 and miR-133; expression of the unintroduced miRNA was unchanged. miR-1 and miR-133 were expressed at levels comparable to those in the adult mouse heart. Error bars reflect one standard deviation.

(C) The population doubling times of mES^{miR-1} and mES$^{miR-133}$ cells were similar to those of control cells. Error bars reflect one standard deviation.

(D) qRT-PCR analyzing expression of *Bry*, an early mesoderm marker, in control, mES^{miR-1}, and mES$^{miR-133}$ EBs collected on day 4 of differentiation. Expression of miR-1 or miR-133 increased expression of *Bry*. Error bars reflect one standard deviation.

(E and F) qRT-PCR analysis of *Nkx2.5* (E) and *Myogenin* (F) expression from day 4, 6, or 10 EBs formed from control, mES^{miR-1}, or mES$^{miR-133}$ cells. Control EBs displayed an induction of *Nkx2.5* expression over time that was enhanced by miR-1 and suppressed by miR-133. Induction of *Myogenin* expression was enhanced by miR-1, but not by miR-133. Error bars reflect one standard deviation.

(G) Differences in *Nkx2.5* expression (green fluorescent cells) were also visualized at day 10 of differentiation by expressing the miRNAs in an *Nkx2.5*-GFP transgenic mES cell line.

(H) Expression of miR-1 and miR-133 was undetectable in day 10 *SRF*$^{-/-}$ EBs by qRT-PCR. Error bars reflect one standard deviation.

(I) Overexpression of miR-1 and, to a lesser extent, miR-133 in *SRF*$^{-/-}$ EBs restored the *Bry* and *Mesp1* downregulation in day 10 EBs typical of wild-type cells.

(J) Expression of *Cd53*, *Cxcl4*, and *Thbs1*, which mark hematopoietic lineages, and of *Mef2c*, which encodes a major regulator of muscle differentiation, was partially rescued in *SRF*$^{-/-}$ EBs upon expression of miR-1 or miR-133.

nonmuscle gene expression. First, we differentiated control, mES^{miR-1}, and mES$^{miR-133}$ ES cells in the presence of recombinant nodal, a potent inducer of endoderm differentiation in mES cells (Vallier et al., 2004; Pfendler et al., 2005). As expected, nodal stimulated expression of the endoderm markers α-*Fetoprotein* (*Afp*) and *Hnf4*α in control EBs (Figures 3A and 3B). These markers were expressed at dramatically lower levels in mES^{miR-1} and mES$^{miR-133}$ EBs than in control EBs, indicating that *miR-1* or *miR-133* can each function as potent repressors of endoderm gene expression during differentiation of pluripotent mES cells (Figures 3A and 3B).

miR-1 and miR-133 Suppress Neural Differentiation from mES Cells

Next, we asked whether miR-1 or miR-133 could also suppress neuroectoderm gene expression from pluripotent mES cells. Control, mES^{miR-1}, and mES$^{miR-133}$ ES cells were differentiated in the presence of retinoic acid (RA), a potent inducer of neural differentiation (Bain et al., 1995; Bain et al., 1996). RA-treated, control EBs expressed high levels of neural cell adhesion molecule 1 (*Ncam1*), a marker of mature neurons, by day 10 of differentiation, but *Ncam1* induction was suppressed in both mES^{miR-1} and mES$^{miR-133}$ EBs (Figure 3C). We also examined expression of *Nestin*, which is restricted largely to neural progenitor cells and is downregulated upon further neural differentiation (Hockfield and McKay, 1985). *Nestin* expression persisted beyond day 10 in mES^{miR-1} and mES$^{miR-133}$ EBs, well after its decline in control EBs, suggesting an accumulation of neural progenitors (Figure 3D). Suppression of endoderm or neuroectoderm differentiation was not observed when an endothelial-enriched microRNA, miR-126, was similarly introduced into mES cells (see Figure S1 available online), indicating specificity of miR-1 and miR-133 effects. These data indicate that both miR-1 and miR-133 can curtail the differentiation of pluripotent cells into mature neurons, even as cells are pushed toward that lineage by timed administration of RA.

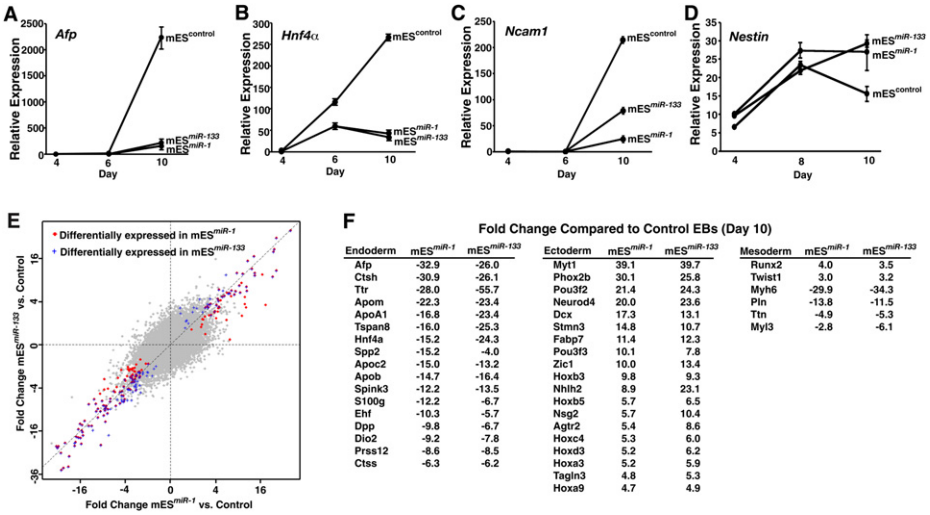

Endoderm	mES^{miR-1}	mES$^{miR-133}$
Afp	-32.9	-26.0
Ctsh	-30.9	-26.1
Ttr	-28.0	-55.7
Apom	-22.3	-23.4
ApoA1	-16.8	-23.4
Tspan8	-16.0	-25.3
Hnf4a	-15.2	-24.3
Spp2	-15.2	-4.0
Apoc2	-15.0	-13.2
Apob	-14.7	-16.4
Spink3	-12.2	-13.5
S100g	-12.2	-6.7
Ehf	-10.3	-5.7
Dpp	-9.8	-6.7
Dio2	-9.2	-7.8
Prss12	-8.6	-8.5
Ctss	-6.3	-6.2

Ectoderm	mES^{miR-1}	mES$^{miR-133}$
Myt1	39.1	39.7
Phox2b	30.1	25.8
Pou3f2	21.4	24.3
Neurod4	20.0	23.6
Dcx	17.3	13.1
Stmn3	14.8	10.7
Fabp7	11.4	12.3
Pou3f3	10.1	7.8
Zic1	10.0	13.4
Hoxb3	9.8	9.3
Nhlh2	8.9	23.1
Hoxb5	5.7	6.5
Nsg2	5.7	10.4
Agtr2	5.4	8.6
Hoxc4	5.3	6.0
Hoxd3	5.2	6.2
Hoxa3	5.2	5.9
Tagln3	4.8	5.3
Hoxa9	4.7	4.9

Mesoderm	mES^{miR-1}	mES$^{miR-133}$
Runx2	4.0	3.5
Twist1	3.0	3.2
Myh6	-29.9	-34.3
Pln	-13.8	-11.5
Ttn	-4.9	-5.3
Myl3	-2.8	-6.1

Figure 3. Both miR-1 and miR-133 Suppress Endoderm and Neuroectoderm Differentiation in mES Cells

(A and B) qRT-PCR analysis of the endoderm markers *Afp* (A) or *Hnf4α* (B) from day 4, 6, or 10 nodal-treated EBs formed from control, mES^{miR-1}, or mES$^{miR-133}$ cells. Induction of *Afp* and *Hnf4α* expression normally observed during differentiation in the presence of nodal was suppressed by expression of miR-1 or miR-133. Error bars reflect one standard deviation.

(C) qRT-PCR analysis of the neural marker *Ncam1* from day 4, 6, or 10 RA-treated EBs formed from control, mES^{miR-1}, or mES$^{miR-133}$ cells. Expression of miR-1 or miR-133 suppressed the induction of *Ncam* normally observed during differentiation in the presence of RA. Error bars reflect one standard deviation.

(D) qRT-PCR analysis of the neural progenitor marker *Nestin* in day 4, 8, or 10 RA-treated EBs formed from control, mES^{miR-1}, or mES$^{miR-133}$ cells. *Nestin* expression declined in wild-type EBs by day 10 as neurons differentiated, but was maintained in mES^{miR-1} and mES$^{miR-133}$ EBs. Error bars reflect one standard deviation.

(E) Plot comparing results from mRNA expression microarray analyses of day 10 control, mES^{miR-1}, and mES$^{miR-133}$ EBs. Plot shows that most genes were coordinately regulated.

(F) Examples of genes that were coordinately regulated in mES^{miR-1} and mES$^{miR-133}$ EBs compared to controls.

Coordinate Dysregulation of Gene Expression in mES^{miR-1} and mES$^{miR-133}$ EBs

To more broadly assess the influence of miR-1 or miR-133 on lineage specification and gene expression, we performed mRNA expression microarray analyses on day 10 control, mES^{miR-1}, and mES$^{miR-133}$ EBs. Consistent with the similar effects of miR-1 and miR-133 on repression of nonmuscle gene expression, the vast majority of genes were coordinately regulated in mES^{miR-1} and mES$^{miR-133}$ EBs (Figure 3E). Among the most highly downregulated genes in both the mES^{miR-1} and mES$^{miR-133}$ EBs were the early endoderm markers, *Afp* and *Hnf4α*, consistent with our qRT-PCR results from EBs treated with nodal (Figure 3F). Expression of other genes normally enriched in endodermal structures, such as those encoding apolipoproteins, was also downregulated in both mES^{miR-1} and mES$^{miR-133}$ EBs (Figure 3F). These results support the idea that miR-1 and miR-133 can suppress endoderm specification and differentiation.

Among the most highly upregulated genes in both mES^{miR-1} and mES$^{miR-133}$ EBs were those associated with neuroectoderm specification and early neural differentiation. These included the early neurogenic transcription factors, *Neurod4*, *Phox2b*, and *Myt1*, and a number of *Hox* genes involved in neural specification (Figure 3F). This is consistent with our observation of persistent *Nestin* expression in mES^{miR-1}- and mES$^{miR-133}$-derived EBs and the apparent disruption of late-stage neuronal differentiation by these miRNAs.

A number of mesodermal genes were also commonly dysregulated in both mES^{miR-1} and mES$^{miR-133}$ EBs (Figure 3F). Runx2 and Twist1, which are highly expressed in developing bone (Ducy et al., 1997; Bialek et al., 2004), were both upregulated, further supporting our conclusion that mesoderm specification is increased in miR-1- or miR-133-expressing EBs. However, a number of genes encoding sarcomeric proteins found in differentiated muscle cells were decreased in both mES^{miR-1} and mES$^{miR-133}$ EBs. The mechanism for diminished sarcomeric gene expression in EBs may differ in the two cells lines: mesodermal progenitors in the mES$^{miR-133}$ EBs likely fail to differentiate into muscle, remaining in the progenitor state, while differentiating muscle cells in mES^{miR-1} EBs may prematurely exit the cell cycle, resulting in fewer cardiac cells, as was observed upon overexpression of miR-1 in the mouse heart (Zhao et al., 2005). Both mechanisms would result in underrepresented muscle gene expression, and each is consistent with our current understanding of miR-1 and miR-133 function.

miR-1 and miR-133 Suppress Neural Differentiation during Teratoma Formation

To examine the ability of miR-1 and miR-133 to suppress nonmesodermal lineages in a more in vivo setting, we injected wild-type or miRNA-expressing mES cells subcutaneously into SCID mice and monitored their differentiation in vivo. Transplanted cells of each line formed teratomas in the recipients and were analyzed 6 weeks after inoculation. Teratomas from control, mES^{miR-1}, or mES$^{miR-133}$ cells included derivatives of all three embryonic germ layers, but the control teratomas were much more homogeneous (Figure 4). As shown by immunostaining with βIII-tubulin antibodies, teratomas from control mES cells were composed mostly of differentiated neurons

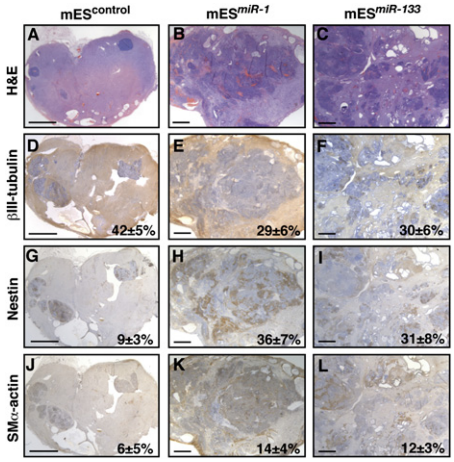

Figure 4. Differentiation of Neural Cells Is Suppressed by miR-1 or miR-133 in Teratomas

Teratomas were generated by injecting control, mES^{miR-1}, or mES$^{miR-133}$ cells into the rear flank of SCID mice. After 6 weeks, hematoxylin and eosin-stained teratomas derived from control ES cells were strikingly homogeneous (A) and composed mostly of βIII-tubulin-immunoreactive neural cells (D). Teratomas from mES^{miR-1} or mES$^{miR-133}$ cells were more heterogeneous (B and C) and contained fewer βIII-tubulin-positive cells (E and F). An accumulation of nestin-positive neural precursors was observed in miR-1- or miR-133-expressing teratomas compared to control (G–I). Expression of miR-1 or miR-133 enhanced muscle specification, as shown by immunostaining with smooth muscle α-actin antibody (J–L). Quantification of areas immunostained with each antibody is indicated as percentages with standard deviation. Scale bars represent ~2 mm.

(Figures 4A and 4D). In contrast, teratomas formed from mES^{miR-1} or mES$^{miR-133}$ cells had far fewer differentiated neuronal cells (Figures 4B, 4C, 4E, and 4F).

Based on our analyses of neural differentiation in EBs, we also immunostained teratomas using an antibody to nestin. Control teratomas were fully differentiated and contained only rare pockets of nestin-positive neural progenitors, as expected (Figure 4G). However, mES^{miR-1} and mES$^{miR-133}$ teratomas contained abundant nestin-positive cells even after 6 weeks of development, suggesting an arrest of neural differentiation at the progenitor stage (Figures 4H and 4I). The accumulation of nestin-positive progenitors in these teratomas further supports the idea that miR-1 and miR-133 permit specification of the ectodermal lineage from pluripotent mES cells but inhibit complete differentiation of neural progenitor cells into neurons.

We also immunostained teratomas using an antibody to smooth muscle α-actin, a marker of smooth muscle and immature striated muscle cells (cardiac and skeletal). Consistent with the promesodermal effects of miR-1 and miR-133 in EBs, mES^{miR-1}- and mES$^{miR-133}$-derived teratomas had more cells on average expressing smooth muscle α-actin (Figures 4K and 4L) than control (Figure 4J). High-magnification views of immunostained sections demonstrate the specificity of each antibody (Figure S2).

The Notch Ligand, Delta-like 1, Is Translationally Repressed by miR-1

miRNAs likely function by regulating numerous pathways, but in some cases a subset serve as the "major" effectors. Since Notch signaling can promote neural differentiation and inhibit muscle differentiation in ES cells (Nemir et al., 2006; Lowell et al., 2006), which is opposite of miR-1's effects, we hypothesized that miR-1-mediated repression of Notch signaling may contribute to the observed effects of miR-1 in mES cells. Indeed, we had previously shown that miR-1 directly targets the Notch ligand *delta* in *Drosophila* for repression (Kwon et al., 2005). Three orthologs of *Drosophila delta* have been identified in mice: *Dll-1*, *Dll-3*, and *Dll-4*. *Dll-1* and *Dll-4*, but not *Dll-3*, contained putative miR-1 or miR-133 binding sites in their 3′ UTR. As shown by qRT-PCR analysis, mRNA expression of *Dll-1* and *Dll-4* was similar in mES^{miR-1} and mES$^{miR-133}$ cells and somewhat higher than in control mES cells (Figure 5A).

Since miRNAs can block the translation of target mRNAs, we examined Dll-1 and Dll-4 protein levels in all three mES cell lines (Figure 5B). mES^{miR-1}, mES$^{miR-133}$, and control cells had similar levels of Dll-4 by immunocytochemistry (Figure 5B) and western analysis (data not shown). Quantitative analysis of endogenous Dll-1 protein was not possible due to the lack of published Dll-1 antibodies that function in western blots. However, mES^{miR-1} cells had consistently decreased Dll-1 protein levels by immunocytochemistry despite having normal levels of *Dll-1* mRNA, consistent with translational inhibition of Dll-1 by miR-1. Although a potential miR-1 binding site in the Dll-1 3′ UTR has extensive, conserved sequence matching (Figure S3A) and is present in an accessible region with little secondary structure (data not shown), repression through this site was not transferable to the luciferase 3′ UTR in the surrogate assay commonly employed to test specific binding sites (Figure S3B). However, miR-1 potently repressed protein, but not mRNA expression of an epitope-tagged Dll-1 containing the full 3′ UTR in a dose-dependent manner, indicating translational inhibition of Dll-1 in mammalian cells (Figure 5C).

Dll-1 Knockdown in mES Cells Promotes Cardiac Mesoderm and Suppresses Nonmesoderm Gene Expression

To determine whether downregulation of Dll-1 protein by miR-1 could account for a subset of the effects of miR-1 on cell lineage decisions, we used short hairpin RNA (shRNA) constructs directed against distinct regions of Dll-1 to generate two different *Dll-1*^{shRNA} cell lines (*Dll-1*$^{shRNA-1}$ and *Dll-1*$^{shRNA-2}$). The *Dll-1* mRNA level was about 62% lower in *Dll-1*$^{shRNA-1}$ cells and 40% lower in *Dll-1*$^{shRNA-2}$ cells than in a control line expressing a scrambled shRNA construct (Figure 5D). *Oct3/4* levels and cell morphology were unaltered (data not shown). EBs formed from *Dll-1*^{shRNA} cells had a much greater propensity toward cardiomyocyte differentiation and formed beating cardiomyocytes earlier than control EBs (Figure 5E). By day 12 of differentiation, 89% of EBs formed from *Dll-1*$^{shRNA-1}$ cells and 97% of EBs from *Dll-1*$^{shRNA-2}$ cells contained beating cardiomyocytes compared to 48% of *Dll-1*^{control} EBs. *Nkx2.5* expression, marking cardiac progenitors, was also more highly induced in *Dll-1*^{shRNA} than in control EBs (Figure 5F), as were Nkx2.5-GFP-positive cells (data not shown). In addition, *Myogenin* expression was higher in *Dll-1*^{shRNA} EBs compared to controls (Figure 5F). Although the effect of Dll-1 knockdown on *Nkx2.5* and *myogenin* expression was not as robust as miR-1 expression, the trends were similar. These results indicate that depletion of Dll-1 increases

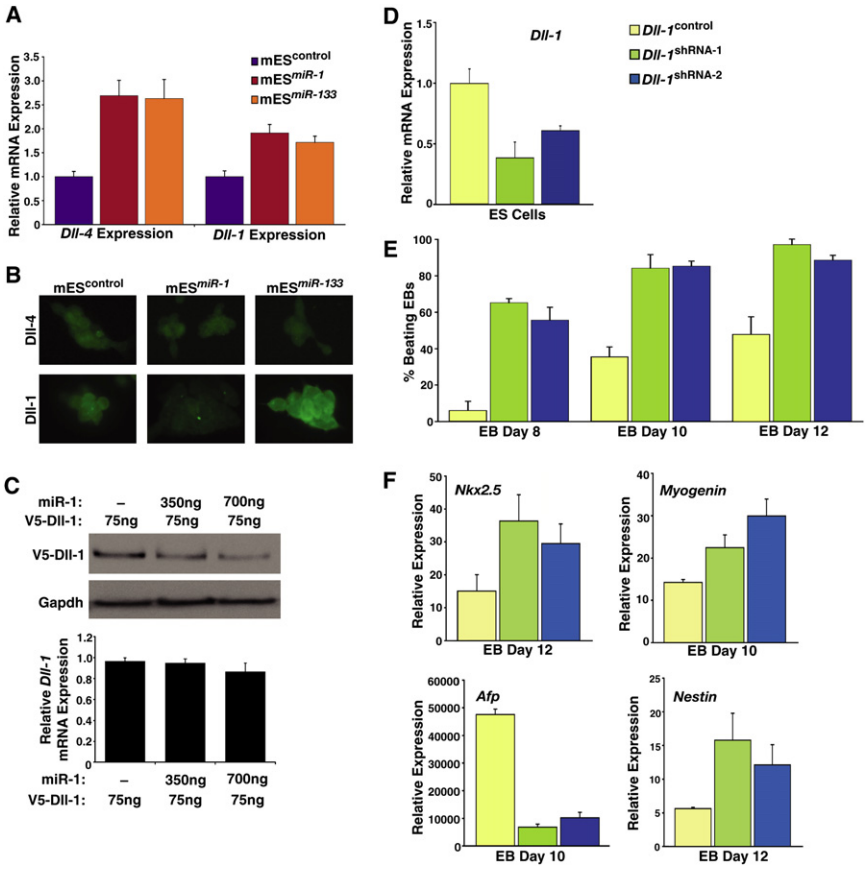

Figure 5. Dll-1 Protein Levels Are Negatively Regulated by miR-1 in mES Cells, and Knockdown of *Dll-1* Expression Promotes Cardiac Mesoderm and Suppresses Nonmesodermal Gene Expression

(A) *Dll-1* and *Dll-4* mRNA levels, assessed by qRT-PCR, were higher in mES^{miR-1} and mES$^{miR-133}$ cells than in controls. Error bars reflect one standard deviation.

(B) Immunostaining with Dll-4 or Dll-1 antibody showed equivalent Dll-4 protein levels in mES^{miR-1}, mES$^{miR-133}$ cells, and control mES cells; Dll-1 protein levels were lower in mES^{miR-1} cells and higher in mES$^{miR-133}$ cells than in wild-type mES cells.

(C) miR-1 expression caused a dose-dependent decrease in epitope (V5)-tagged Dll-1 protein levels by western blot without affecting RNA expression of *Dll-1* assessed by qRT-PCR (graph). Gapdh protein levels reflect equal loading of protein. Error bars reflect one standard deviation.

(D) *Dll-1* mRNA levels, assessed by qRT-PCR, were 62% and 40% lower in response to two distinct short hairpin RNAs targeting *Dll-1* mRNA (*Dll-1*$^{shRNA-1}$ and *Dll-1*$^{shRNA-2}$) than in a control cell line. Error bars reflect one standard deviation.

(E) EBs formed from *Dll-1*^{control}, *Dll-1*$^{shRNA-1}$, and *Dll-1*$^{shRNA-2}$ ES cells were scored for beating cardiomyocytes on days 8, 10, and 12 of differentiation. Beating cardiomyocytes appeared earlier and were more numerous in EBs from *Dll-1*^{shRNA} cell lines than in EBs from the control line. Error bars reflect one standard deviation.

(F) qRT-PCR analyses of *Nkx2.5*, *Myogenin*, *Afp*, and *Nestin* expression in EBs generated from *Dll-1*^{control}, *Dll-1*$^{shRNA-1}$, and *Dll-1*$^{shRNA-2}$ ES cells. Knocking down *Dll-1* increased *Myogenin* expression, decreased *Afp* expression, and sustained *Nestin* expression compared to controls, relative to ES cells. Error bars reflect one standard deviation.

muscle differentiation from mES cells and suggest that miR-1 may promote cardiac differentiation, in part, by downregulating Dll-1 protein.

We also performed qRT-PCR analyses on EBs formed from *Dll-1*^{shRNA} cell lines to determine if suppression of ectodermal and endodermal lineages by *miR-1* might also involve Dll-1 downregulation. Expression of the endoderm markers *Afp* (Figure 5F) and *Hnf4*α (data not shown) was lower in *Dll-1*^{shRNA} EBs than in *Dll-1*^{control} EBs. Moreover, expression of *Nestin*, which decreased between days 10 and 12 as neurons differentiated in *Dll-1*^{control} EBs, was increased during this period in both lines of *Dll-1*^{shRNA} EBs (Figure 5F). Thus, loss of Dll-1 also represses endoderm differentiation and results in persistence of neural progenitor gene expression.

Effects of miR-1 or miR-133 in Human ES Cells

Human ES (hES) cells often behave differently from mES cells. To investigate whether miR-1 or miR-133 function similarly in the two cell types, we infected the H9 hES cell line with the same lentiviruses encoding either miR-1 or miR-133. Expression was verified by qRT-PCR (Figure 6A). The resulting hES^{miR-1} and hES$^{miR-133}$ cell lines were differentiated as EBs in suspension and collected on days 4, 6, and 8. *NKX2.5* expression was detectable by qRT-PCR in control human EBs by day 6 and decreased overall by day 8 (Figure 6B). As in the mouse EBs, hES^{miR-1} EBs had higher levels of *NKX2.5* expression than controls, while hES$^{miR-133}$ EBs failed to induce *NKX2.5* expression to the levels observed in controls (Figure 6B). Consistent with this finding, the percentage of hES^{miR-1} EBs with beating cardiac cells on day 18 of differentiation was more than 3-fold higher than in wild-type EBs, while hES$^{miR-133}$ EBs did not display enhanced cardiomyocyte formation (Figure 6C). Thus, regulation of cardiac differentiation by miR-1 and miR-133 appears to be grossly similar in hES and mES cells.

To examine the effects of miR-1 or miR-133 expression on neuroectoderm differentiation in hES cells, we also immunostained day 18 control, hES^{miR-1}, and hES$^{miR-133}$ EBs with antibodies recognizing nestin or βIII-tubulin (Figure 6D). Like miRNA-expressing mouse EBs, hES^{miR-1} and hES$^{miR-133}$ EBs accumulated more nestin-positive progenitors than control human EBs. As in our mouse ES cell studies, there were fewer βIII-tubulin-positive neural cells in hES$^{miR-133}$ EBs compared to controls, although this effect was not consistently observed in hES^{miR-1} cells. These results demonstrate that the muscle-specific miRNAs miR-1 and miR-133 have similar, but unique, effects on the differentiation of hES and mES cells and suggest that miRNAs may be useful for coaxing and repressing differentiation of human or mouse ES cells into particular lineages.

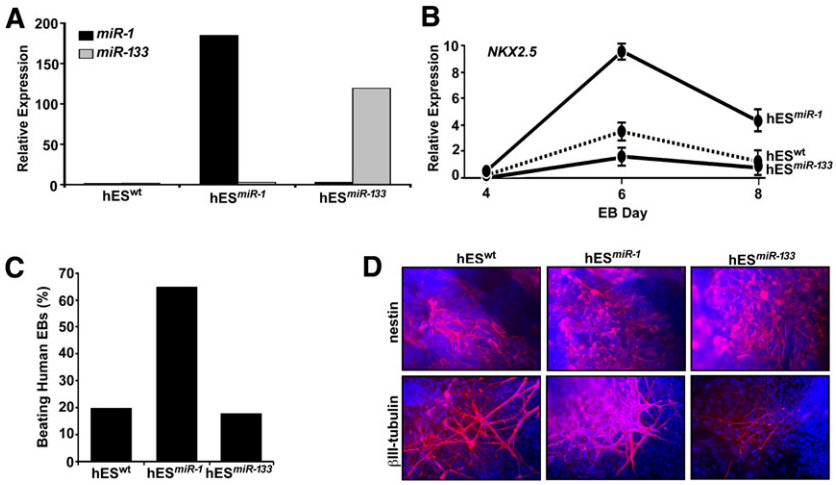

Figure 6. Effects of miR-1 or miR-133 Expression in hES Cells

(A) Lentivirus-mediated expression of miR-1 or miR-133 in human ES (hES) cells was verified by qRT-PCR.

(B) *NKX2.5* mRNA expression assessed by qRT-PCR in hEBs collected on days 4, 6, and 8. Overexpression of miR-1 in hES cells increased *NKX2.5* expression compared to wild-type, while *miR-133* expression led to decreased *NKX2.5* induction. Error bars reflect one standard deviation.

(C) Human EBs were scored for beating on day 18 of differentiation. Expression of miR-1 increased the number of beating human EBs, while expression of miR-133 did not.

(D) Day 18 human EBs were immunostained with antibodies to nestin or βIII-tubulin.

DISCUSSION

This study shows that miR-1 can promote differentiation of both mouse and human ES cells into the cardiac lineage, while miR-133, which is normally coexpressed with miR-1 in developing muscle, blocks differentiation of myogenic precursors. Both miRNAs enhanced mesoderm specification and suppressed the differentiation of ES cells into neuroectoderm or endoderm within EBs or teratomas. miR-1 expression resulted in translational repression of Dll-1, a mammalian ortholog of *delta*, and reducing the level of Dll-1 expression in mES cells using shRNAs caused similar cell fate trends as miR-1 expression.

The onset of miR-1 and miR-133 expression in mES cells occurred just as mesoderm is becoming specified at day 4, consistent with the early *twist*-dependent expression of *miR-1* throughout *Drosophila* mesoderm, preceding *mef2* expression (Kwon et al., 2005; Sokol and Ambros, 2005). The ability of miR-1 and miR-133 to promote early mesoderm gene expression when misexpressed suggests that this early onset in ES cells may promote mesoderm lineages. Strikingly, further differentiation of mesoderm into the muscle lineage was promoted by miR-1 but inhibited by miR-133. This is similar to in vivo observations (Zhao et al., 2005; Chen et al., 2006).

The findings in $SRF^{-/-}$ ES cells that do not express miR-1 or miR-133 provide important data that compliment the gain-of-function studies. $SRF^{-/-}$ cells are known to have a block of final muscle differentiation (Weinhold et al., 2000), but the persistence of *Bry* expression, indicative of an arrest of early mesodermal progenitors, had not been noted. This observation allowed us to determine whether loss of miR-1/miR-133 transcription in $SRF^{-/-}$ cells might play a causative role in this interesting developmental block. The ability of miR-1 to rescue the further differentiation of mesodermal progenitors suggests that it can push arrested mesoderm in $SRF^{-/-}$ ES cells past the stage of *Bry* expression, although it did not induce sarcomeric gene expression.

Unexpectedly, miR-1 and miR-133 potently repressed endoderm and neuroectoderm gene expression. This repression was observed during in vitro differentiation experiments, despite the presence of potent inducers of each lineage, and during teratoma formation in vivo. In contrast to their roles during muscle differentiation, miR-1 and miR-133 functioned in concert to repress nonmuscle gene expression, suggesting that they may have many common targets, although competitive increases in mesoderm specification may account for some of the observed alternative lineage suppression. Gene expression analyses of ES cells expressing miR-1 and miR-133 also suggested that the two microRNAs regulate many pathways in common. To our knowledge, this is the first example in which miR-1 and miR-133 function in a parallel rather than opposing fashion, consistent with their bicistronic derivation. Nonmuscle gene expression was not detected in *miR-1-2* null mouse hearts (data not shown). However, conclusively determining whether miR-1 is required to repress nonmuscle gene expression in vivo awaits the creation of compound miR-1-1 and miR-1-2 knockout mice.

The combined effects of the miRNAs in regulating mesoderm differentiation and preventing endoderm and neuroectoderm differentiation reflect a novel but elegant mechanism for controlling lineage decisions (Figure 7). By initiating the expression of specific miRNAs, a cell might promote active clearance of transcripts that it has "outgrown" and expedite further differentiation. The repression of undesired gene expression may also be useful in efforts to differentiate and utilize ES cells for therapeutic purposes, as strict control of lineage potential is of utmost concern to avoid tumor formation and introduction of harmful cell types.

Several targets for miR-1 and some for miR-133 have been described, and scores more have been predicted but not validated. Therefore, it is likely that these miRNAs control cell-fate decisions by regulating numerous genes and pathways. miR-1 regulated the translation of Dll-1 protein, thereby negatively influencing Notch signaling, consistent with the observation that miR-1 negatively regulates Notch signaling by targeting *delta* in *Drosophila*. Specific knockdown of Dll-1 caused cell-fate trends similar to those caused by miR-1 expression, although combinatorial targeting of multiple mRNAs likely results in the full effect of miR-1. Consistent with the effects of miR-1 expression and Dll-1 knockdown, recent reports indicate that Notch1 inhibition promotes cardiac differentiation and that stimulation of the Notch pathway positively regulates neuronal differentiation (Nemir et al., 2006; Lowell et al., 2006). Thus, despite the many pathways likely repressed by miR-1, our findings suggest that

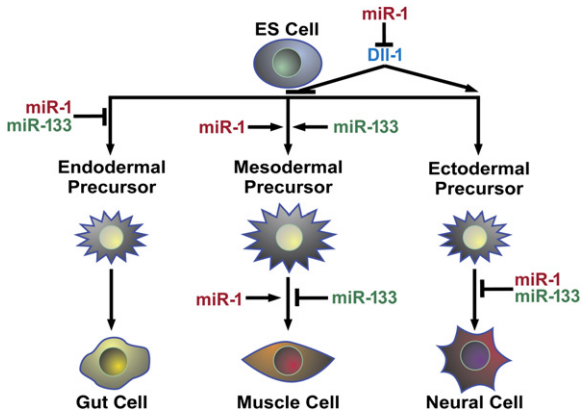

Figure 7. Model of miR-1/miR-133 Effects during ES Cell Differentiation

miR-1 and miR-133 promotion of mesoderm and inhibition of endoderm and ectoderm differentiation at specific stages are indicated. Opposing effects of the two miRNAs in later steps of muscle differentiation are also shown. miR-1 inhibition of Dll-1 translation, along with yet unknown targets, likely contribute to some of the observed effects of miR-1.

negative regulation of Notch signaling may be one of the major mechanisms by which miR-1 influences cell fate decisions (Figure 7). Whether miR-133 also functions by regulating other components of Notch signaling or whether it targets independent pathways remains to be determined. It will be interesting to determine if miR-1 or miR-133 also control other regulators of cardiac progenitors such as those involved in canonical Wnt signaling (Kwon et al., 2007).

In summary, our results indicate that the muscle-specific miRNAs miR-1 and miR-133 act comparably during mES and hES differentiation to promote mesoderm differentiation while suppressing gene expression of alternative lineages. Our results also suggest that miRNAs may offer a means to direct the differentiation of ES cells into desired fates and inhibit the formation of undesired lineages.

EXPERIMENTAL PROCEDURES

Mouse ES Cell Culture and Flow Cytometry

The mouse E14 ES cell line was maintained as a monolayer in medium supplemented with 10% fetal bovine serum, LIF-conditioned medium, pyruvate, glutamine, and β-mercaptoethanol in gelatin-coated tissue-culture plates and passaged with trypsin. Cells were differentiated by the hanging drop method. Briefly, cells were trypsinized and resuspended at 25,000 cells/ml in differentiation medium (20% fetal bovine serum, pyruvate, glutamine, and β-mercaptoethanol). Droplets (20 μl) were transferred to each well of a 96-well v-bottom tissue culture plate, which was then inverted. After 2 days of incubation at 37°C, the plates were turned upright, and 200 μl of differentiation medium was added to each well. For neuroectodermal or endodermal induction, 0.5 μM retinoic acid (Sigma) or 50 ng/ml recombinant nodal (R&D Systems), respectively, was added to the wells 96 hr after formation of the hanging drops. The medium was changed every 2 days. The β-myosin heavy-chain-GFP E14 cells were a gift of W. Tingley and R. Shaw. For flow cytometry studies, EBs were dissociated with trypsin and passed through a nylon cell strainer. Flk-1$^+$ cells were labeled with a PE-conjugated Flk-1 antibody (BD PharMingen) and a Becton Dickinson (Franklin Lakes, NJ) FACS Diva flow cytometer, and cell sorter was used for detecting and sorting Flk-1$^+$, Nkx2.5-GFP$^+$, or βMHC-GFP$^+$ cells.

miRNA and mRNA Expression Microarray Analyses

ES cells or EBs were harvested in Trizol (Invitrogen) for total RNA isolation. For mRNA expression microarray analysis, 1 μg total RNA was labeled and hybridized to a mouse mRNA expression microarray (Affymetrix). Gene expression values were obtained from Affymetrix CEL files using the GC-RMA package from Bioconductor (Dudoit et al., 2003; Wu and Irizarry, 2004). To identify transcripts differing in mean expression across the three experimental groups (mES^{wt}, mES^{miR-1}, and mES$^{miR-133}$ EBs), p values were calculated by permutation test with the F-statistic function from the multitest package of Bioconductor (Dudoit et al., 2003) and a t test comparing each miRNA-expressing group to wild-type EBs. Fold changes in transcript levels were calculated from the mean log2 expression values versus the mean of control EBs.

For miRNA expression microarray, 100 ng of total RNA from each sample was labeled with Cy3 or Cy5 using miRCURY LNA microRNA Power labeling kit (Exiqon) and then hybridized to miRCURY LNA arrays (Exiqon). Hybridization quality was assessed with Bioconductor *marray* package, and log2 ratios of Cy5 to Cy3 signals were calculated with *limma* package.

Quantitative RT-PCR

ES cells or EBs were harvested in Trizol (Invitrogen) for total RNA isolation. For mRNA qRT-PCR, 2 μg of total RNA from each sample was reversed transcribed with Superscript III (Invitrogen). One-sixteenth of the reverse transcription reaction was used for subsequent PCRs, which were performed in duplicate on an ABI 7900HT instrument (Applied Biosystems) using Taqman primer probe sets (Applied Biosystems) for each gene of interest and a GAPDH endogenous control primer probe set for normalization. Each qRT-PCR was performed on at least three different experimental samples; representative results are shown as fold expression relative to undifferentiated ES cells unless otherwise stated. Error bars reflect one standard deviation from the mean of technical replicates.

miRNA qRT-PCR was performed with miRNA Taqman Expression Assays (Applied Biosystems) and the miRNA Reverse Transcription kit (Applied Biosystems). For each miRNA analyzed, 10 ng of total RNA was reverse transcribed with a miRNA-specific primer. A ubiquitous miRNA, miR-16, was used as the endogenous control. Each qRT-PCR was performed on at least three different experimental samples; representative results are shown as fold expression relative to undifferentiated ES cells unless otherwise noted. Error bars indicate one standard deviation from the mean of technical replicates.

Lentiviral Production and ES Cell Infection

Lentiviruses for miRNA expression were generated with the ViraPower Promoterless Lentiviral Gateway Expression System with MultiSite Gateway Technology (Invitrogen). The *EF-1α* promoter was recombined into the pLenti vector upstream of a cassette containing either miR-1 or miR-133 pre-miRNA sequence with an additional ~100 nucleotides flanking each end, which was cloned by PCR from a bacterial artificial chromosome containing the mouse genomic *miR-1-2 or miR-133a-1* sequences. Details of virus production and introduction into ES cells can be found in the Supplemental Experimental Procedures.

Teratoma Formation

Teratomas were formed by subcutaneous injection of approximately 1×10^6 control or miRNA-expressing mES cells into the rear flank of 8-week-old male SCID mice (n = 10 mice per cell line). Transplanted cells of each line formed teratomas in the recipients and were analyzed 6 weeks after inoculation.

Immunostaining

For immunocytochemistry studies, ES cells were plated on gelatinized coverslips and allowed to settle, rinsed with PBS, fixed in 4% paraformaldehyde for 1 hr at room temperature with shaking, and stored in PBS at 4°C. The fixed cells were rinsed in PBS, blocked in blocking solution (1% bovine serum albumin, 1% Tween-20, and PBS) for 30 min at room temperature and incubated in primary antibody in a humidified chamber for 1 hr at room temperature. The antibodies were diluted in blocking buffer as follows: Dll-1, 1:100 (AbCam, ab10554); Jag-1, 1:100 (AbCam, ab7771); Dll-4, 1:50 (AbCam, ab7280). After washing in PBS, the cells were incubated for 1 hr with FITC-conjugated secondary antibodies (1:200) at room temperature in a darkened chamber, rinsed

with PBS, and mounted on slides with Vectashield containing DAPI (Vector Laboratories).

For immunohistochemical studies, teratomas were submerged in CPT (Sakuro), flash frozen in liquid nitrogen, and sectioned. Details of immunostaining and antibodies are in the Supplemental Experimental Procedures.

For EB immunohistochemistry, EBs were fixed in 4% paraformaldehyde, blocked in 5% goat serum, and incubated overnight in βIII-tubulin antibody (1:100; Chemicon, CBL412). The following day, EBs were rinsed, placed in rhodamine-conjugated anti-mouse IgG diluted 1:400 for 2 hr, rinsed, mounted with Vectashield containing DAPI (Vector Laboratories), and visualized.

Dll-1 Knockdown

mES cells were infected with lentiviral constructs encoding shRNAs against mouse *Dll-1* or a control shRNA (Sigma). After transduction and 2 days of recovery, infected mES cells were selected for 7 days with 1 μg/ml puromycin. Colonies were isolated, expanded, and assayed for *Dll-1* knockdown compared to control-infected mES cells by qRT-PCR. The pluripotency of the resulting cell lines was assessed by measuring the proliferation rate and *Oct3/4* expression and comparing the value to those of uninfected mES cells. Only lines that maintained normal levels of *Oct3/4* expression and normal proliferation rates were used for further study.

miR-1 Target Analyses

For luciferase assays or transient expression analyses, Cos-1 cells in 12-well plates were transfected with Lipofectamine 2000 (Invitrogen). For luciferase assays, a luciferase expression construct containing the 3′ UTR of mouse Dll-1 (50 ng) was cotransfected alone or with miR-1 or miR-133 expression constructs (300 ng) and a *LacZ* expression construct. Empty expression plasmid was used to normalize the total DNA mass. After 24 hr, cells were harvested and the luciferase assays were performed with Luciferase Assay Kit (Promega). β-galactosidase assays were also performed and the results were used to normalize for transfection efficiency. For transient expression analyses, a Dll-1 expression construct lacking Dll-1-derived 5′ UTR sequence elements, but with the full mouse Dll-1 3′ UTR, and an n-terminal V5 epitope tag (75 ng) was cotransfected with increasing amounts of miR-1 expression construct (0 ng, 350 ng, or 700 ng). Empty expression vector was included to ensure equal DNA mass in each condition. After 24 hr, cells were harvested in modified RIPA buffer or Trizol (Invitrogen). Western analyses to detect V5-tagged Dll-1 protein were performed with HRP-conjugated V5 antibody diluted 1:1500 (Invitrogen).

Human ES Cell Culture

The human ES cell line, H9 (WiCell), was maintained on mouse embryonic feeder cells in proliferation medium consisting of Knockout DMEM (GIBCO) supplemented with 20% Knockout serum replacement (GIBCO), pyruvate, glutamine, β-mercaptoethanol and human basic fibroblast growth factor. Details of hES cell differentiation and immunostaining can be found in Supplemental Experimental Procedures.

SUPPLEMENTAL DATA

The Supplemental Data include three figures and Supplemental Experimental Procedures and can be found with this article online at http://www.cellstemcell.com/cgi/content/full/2/3/219/DC1/.

ACKNOWLEDGMENTS

We are grateful to members of the Srivastava lab and to B.G. Bruneau for critical discussion and comments on the manuscript; to B. Taylor and G. Howard for editorial assistance and manuscript preparation; to C. Barker and the Gladstone Genomics core and J. Fish. in the Histopathology core for technical assistance; to W. Tingley and R. Shaw for sharing the β-MHC ES cell line; and to N. Salomonis for assistance with microarray data analysis. D.S. is supported by grants from NHLBI/NIH, March of Dimes Birth Defects Foundation, and the California Institute of Regenerative Medicine and is an Established Investigator of the American Heart Association. K.N.I. is a postdoctoral scholar of the California Institute of Regenerative Medicine (T2-0003), and her work is supported by the Lynda and Stuart Kesnick Foundation. H.S.B. was supported by a grant from NHLBI/NIH (HL085377), and F.W.K. was supported by NRSA/NIH (HL007544). This work was also supported by NIH/NCRR grant (C06RR018928) to the Gladstone Institutes.

Received: October 12, 2007
Revised: January 9, 2008
Accepted: January 24, 2008
Published: March 5, 2008

REFERENCES

Ambros, V. (2004). The functions of animal microRNAs. Nature *431*, 350–355.

Bain, G., Kitchens, D., Yao, M., Huettner, J.E., and Gottlieb, D.I. (1995). Embryonic stem cells express neuronal properties in vitro. Dev. Biol. *168*, 342–357.

Bain, G., Ray, W.J., Yao, M., and Gottlieb, D.I. (1996). Retinoic acid promotes neural and represses mesodermal gene expression in mouse embryonic stem cells in culture. Biochem. Biophys. Res. Commun. *223*, 691–694.

Bialek, P., Kern, B., Yang, X., Schrock, M., Sosic, D., Hong, N., Wu, H., Yu, K., Ornitz, D.M., Olson, E.N., et al. (2004). A twist code determines the onset of osteoblast differentiation. Dev. Cell *6*, 423–435.

Chen, J.F., Mandel, E.M., Thomson, J.M., Wu, Q., Callis, T.E., Hammond, S.M., Conlon, F.L., and Wang, D.Z. (2006). The role of microRNA-1 and microRNA-133 in skeletal muscle proliferation and differentiation. Nat. Genet. *38*, 228–233.

Ducy, P., Zhang, R., Geoffroy, V., Ridall, A.L., and Karsenty, G. (1997). Osf2/Cbfa1: A transcriptional activator of osteoblast differentiation. Cell *89*, 747–754.

Dudoit, S., Gentleman, R.C., and Quackenbush, J. (2003). Open source software for the analysis of microarray data. Biotechniques (*Suppl*), 45–51.

He, L., and Hannon, G.J. (2004). MicroRNAs: Small RNAs with a big role in gene regulation. Nat. Rev. Genet. *5*, 522–531.

Hockfield, S., and McKay, R.D. (1985). Identification of major cell classes in the developing mammalian nervous system. J. Neurosci. *5*, 3310–3328.

Hornstein, E., Mansfield, J.H., Yekta, S., Hu, J.K., Harfe, B.D., McManus, M.T., Baskerville, S., Bartel, D.P., and Tabin, C.J. (2005). The microRNA miR-196 acts upstream of Hoxb8 and Shh in limb development. Nature *438*, 671–674.

Houbaviy, H.B., Murray, M.F., and Sharp, P.A. (2003). Embryonic stem cell-specific MicroRNAs. Dev. Cell *5*, 351–358.

Kanellopoulou, C., Muljo, S.A., Kung, A.L., Ganesan, S., Drapkin, R., Jenuwein, T., Livingston, D.M., and Rajewsky, K. (2005). Dicer-deficient mouse embryonic stem cells are defective in differentiation and centromeric silencing. Genes Dev. *19*, 489–501.

Kuehbacher, A., Urbich, C., Zeiher, A.M., and Dimmeler, S. (2007). Role of Dicer and Drosha for endothelial microRNA expression and angiogenesis. Circ. Res. *101*, 59–68.

Kwon, C., Han, Z., Olson, E.N., and Srivastava, D. (2005). MicroRNA1 influences cardiac differentiation in Drosophila and regulates Notch signaling. Proc. Natl. Acad. Sci. USA *102*, 18986–18991.

Kwon, C., Arnold, J., Hsiao, E.C., Taketo, M.M., Conklin, B.R., and Srivastava, D. (2007). Canonical Wnt signaling is a positive regulator of mammalian cardiac progenitors. Proc. Natl. Acad. Sci. USA *104*, 10894–10899.

Loebel, D.A., Watson, C.M., De Young, R.A., and Tam, P.P. (2003). Lineage choice and differentiation in mouse embryos and embryonic stem cells. Dev. Biol. *264*, 1–14.

Lowell, S., Benchoua, A., Heavey, B., and Smith, A.G. (2006). Notch promotes neural lineage entry by pluripotent embryonic stem cells. PLoS Biol. *4*, e121. 10.1371/journal.pbio.0040121.

Maltsev, V.A., Wobus, A.M., Rohwedel, J., Bader, M., and Hescheler, J. (1994). Cardiomyocytes differentiated in vitro from embryonic stem cells developmentally express cardiac-specific genes and ionic currents. Circ. Res. *75*, 233–244.

Molkentin, J.D., Black, B.L., Martin, J.F., and Olson, E.N. (1995). Cooperative activation of muscle gene expression by MEF2 and myogenic bHLH proteins. Cell *83*, 1125–1136.

Murchison, E.P., Partridge, J.F., Tam, O.H., Cheloufi, S., and Hannon, G.J. (2005). Characterization of Dicer-deficient murine embryonic stem cells. Proc. Natl. Acad. Sci. USA *102*, 12135–12140.

Nemir, M., Croquelois, A., Pedrazzini, T., and Radtke, F. (2006). Induction of cardiogenesis in embryonic stem cells via downregulation of Notch1 signaling. Circ. Res. *98*, 1471–1478.

Niu, Z., Yu, W., Zhang, S.X., Barron, M., Belaguli, N.S., Schneider, M.D., Parmacek, M., Nordheim, A., and Schwartz, R.J. (2005). Conditional mutagenesis of the murine serum response factor gene blocks cardiogenesis and the transcription of downstream gene targets. J. Biol. Chem. *280*, 32531–32538.

Pfendler, K.C., Catuar, C.S., Meneses, J.J., and Pedersen, R.A. (2005). Overexpression of Nodal promotes differentiation of mouse embryonic stem cells into mesoderm and endoderm at the expense of neuroectoderm formation. Stem Cells Dev. *14*, 162–172.

Rao, P.K., Kumar, R.M., Farkhondeh, M., Baskerville, S., and Lodish, H.F. (2006). Myogenic factors that regulate expression of muscle-specific microRNAs. Proc. Natl. Acad. Sci. USA *103*, 8721–8726.

Saga, Y., Hata, N., Kobayashi, S., Magnuson, T., Seldin, M.F., and Taketo, M.M. (1996). Mesp1: A novel basic helix-loop-helix protein expressed in the nascent mesodermal cells during mouse gastrulation. Development *122*, 2769–2778.

Sokol, N.S., and Ambros, V. (2005). Mesodermally expressed Drosophila microRNA-1 is regulated by Twist and is required in muscles during larval growth. Genes Dev. *19*, 2343–2354.

Srivastava, D., Thomas, T., Lin, Q., Kirby, M.L., Brown, D., and Olson, E.N. (1997). Regulation of cardiac mesodermal and neural crest development by the bHLH transcription factor, dHAND. Nat. Genet. *16*, 154–160.

Srivastava, D. (2006). Making or breaking the heart: From lineage determination to morphogenesis. Cell *126*, 1037–1048.

Vallier, L., Reynolds, D., and Pedersen, R.A. (2004). Nodal inhibits differentiation of human embryonic stem cells along the neuroectodermal default pathway. Dev. Biol. *275*, 403–421.

Wang, Y., Medvid, R., Melton, C., Jaenisch, R., and Blelloch, R. (2007). DGCR8 is essential for microRNA biogenesis and silencing of embryonic stem cell self-renewal. Nat. Genet. *39*, 380–385.

Weinhold, B., Schratt, G., Arsenian, S., Berger, J., Kamino, K., Schwarz, H., Ruther, U., and Nordheim, A. (2000). Srf(−/−) ES cells display non-cell-autonomous impairment in mesodermal differentiation. EMBO J. *19*, 5835–5844.

Wu, Z., and Irizarry, R.A. (2004). Preprocessing of oligonucleotide array data. Nat. Biotechnol. *22*, 656–658, author reply 658.

Yamagishi, H., Yamagishi, C., Nakagawa, O., Harvey, R.P., Olson, E.N., and Srivastava, D. (2001). The combinatorial activities of Nkx2.5 and dHAND are essential for cardiac ventricle formation. Dev. Biol. *239*, 190–203.

Zhao, Y., Samal, E., and Srivastava, D. (2005). Serum response factor regulates a muscle-specific microRNA that targets Hand2 during cardiogenesis. Nature *436*, 214–220.

Zhao, Y., and Srivastava, D. (2007). A developmental view of microRNA function. Trends Biochem. Sci. *32*, 189–197.

Zhao, Y., Ransom, J.F., Li, A., Vedantham, V., von Drehle, M., Muth, A.N., Tsuchihashi, T., McManus, M.T., Schwartz, R.J., and Srivastava, D. (2007). Dysregulation of cardiogenesis, cardiac conduction, and cell cycle in mice lacking miRNA-1–2. Cell *129*, 303–317.